

April 2006

# Polarization reorientation in ferroelectric lead zirconate titanate thin films with electron beams

D. B. Li
*University of Pennsylvania*

Douglas R. Strachan
*University of Pennsylvania*

J. H. Ferris
*University of Pennsylvania*

Dawn A. Bonnell
*University of Pennsylvania*, bonnell@lrsm.upenn.edu



Copyright Materials Research Society. Reprinted from *Journal of Materials Research*, Volume 21, Issue 4, April 2006, pages 935-940. Publisher URL: http://dx.doi.org/10.1557/JMR.2006.0107

# Polarization reorientation in ferroelectric lead zirconate titanate thin films with electron beams

**Abstract**

Ferroelectric domain patterning with an electron beam is demonstrated. Polarization of lead zirconate titanate thin films is shown to be reoriented in both positive and negative directions using piezoresponse force and scanning surface potential microscopy. Reorientation of the ferroelectric domains is a response to the electric field generated by an imbalance of electron emission and trapping at the surface. A threshold of 500 $\mu C/cm^2$ and a saturation of 1500 $\mu C/cm^2$ were identified. Regardless of beam energy, the polarization is reoriented negatively for beam currents less than 50 pA and positively for beam currents greater than 1 nA.

# Polarization reorientation in ferroelectric lead zirconate titanate thin films with electron beams

D.B. Li
*Department of Materials Science and Engineering, University of Pennsylvania, Philadelphia, Pennsylvania 19104*

D.R. Strachan
*Department of Physics and Astronomy and Department of Materials Science and Engineering, University of Pennsylvania, Philadelphia, Pennsylvania 19104*

J.H. Ferris and D.A. Bonnell[a)]
*Department of Materials Science and Engineering, University of Pennsylvania, Philadelphia, Pennsylvania 19104*

(Received 15 September 2005; accepted 5 January 2006)

Ferroelectric domain patterning with an electron beam is demonstrated. Polarization of lead zirconate titanate thin films is shown to be reoriented in both positive and negative directions using piezoresponse force and scanning surface potential microscopy. Reorientation of the ferroelectric domains is a response to the electric field generated by an imbalance of electron emission and trapping at the surface. A threshold of 500 $\mu C/cm^2$ and a saturation of 1500 $\mu C/cm^2$ were identified. Regardless of beam energy, the polarization is reoriented negatively for beam currents less than 50 pA and positively for beam currents greater than 1 nA.

## I. INTRODUCTION

Ferroelectric domain switching, also referred to as polarization reversal or reorientation, in thin films has traditionally attracted attention due to applications in nonvolatile storage devices.[1,2] Recently, a new process for fabricating complex nanostructures based on ferroelectric domain patterning has shown promise.[3,4] In these and other applications, domain reorientation and patterning are accomplished by applying an electric field with macroscopic or patterned metal electrodes or with a metallic scanning probe microscope tip.[5–7] The latter is particularly effective for producing nanometer-sized features with desired polarization orientation. An alternative process for patterning small scale domains is based on e-beam induced polarization reorientation. Ferris et al. produced nanometer-sized domain patterns on polycrystalline lead zirconate titanate (PZT) thin films,[8] and earlier studies produced macroscopic features on single-crystal $LiNbO_3$[9,10] by e-beam irradiation.

When an insulator surface is irradiated by electrons with energy higher than 1 keV, elastic and inelastic collisions in the crystal lead to the excitation of secondary electrons and the backscattering of incident electrons. Secondary electrons that are sufficiently close to the surface (less than 50 nm) are emitted from the surface, while the other electrons are either trapped in defect sites or self-trapped as polarons in the crystal. When the number of incident electrons is not equal to that of the emitted electrons, charge develops and an internal local electrical field is established in the film. When the field generated by the trapped charges is stronger than the coercive field of the ferroelectric compound, domain reorientation at the surface should occur.

While domain reorientation by e-beam irradiation has been demonstrated for the two cases mentioned above, quantitative aspects of the mechanism are not known. For example, excitation cross sections are beam energy dependent, which implies that surface charging will also be energy dependent. This dependence is documented for many compounds from scanning electron microscopy studies[11] but is not determined for ferroelectric compounds. Both transient and steady-state dynamics are related to dosage, and these effects have not been examined. In this paper, we determine the dosage, energy, and current density dependence of polarization reorientation in polycrystalline PZT thin films and relate them to the mechanism of poling.

## II. EXPERIMENTAL PROCEDURE

PZT has the perovskite structure with $Ti^{4+}$ ions and $Zr^{4+}$ ions occupying B-sites with random distribution. At a Zr/Ti-ratio of 53/47, the composition corresponding to

a)Address all correspondence to this author.
e-mail: bonnell@lrsm.upenn.edu
DOI: 10.1557/JMR.2006.0107

  

morphotropic phase transition, PZT has the highest dielectric constant and piezoelectric coefficient.[12] Polycrystalline PZT thin films with a thickness of 160 nm and average grain size of 100 nm were prepared by a sol-gel process on Pt/Ti/$SiO_2$/Si substrates. The composition of the film was $Pb(Zr_{0.53}Ti_{0.47})O_3$; a 10 nm Pt layer was used as the back electrode.[13] Piezoresponse force microscopy (PFM) confirmed that the PZT grains exhibited random polarization orientation.

A scanning electron microscope (SEM) equipped with a $LaB_6$ filament and commercial lithography system was used for ferroelectric domain pattering. The experimental setup is shown in Fig. 1. PZT samples were grounded on the sample stage in the vacuum chamber, which maintained a pressure less than $1 \times 10^{-6}$ Torr during electron irradiation. Focused electron beam energies ranged from 1 to 30 keV and currents ranged from a few pA to tens of nanoampere (nA). Electron beam dosage, beam energy, and beam current were independently adjusted to determine the relationship between polarization reorientation and ferroelectric lithography conditions. Although nanometer scale patterning is possible with this instrumentation, exposure areas in this study were on the order of micrometers to minimize the measurement error.

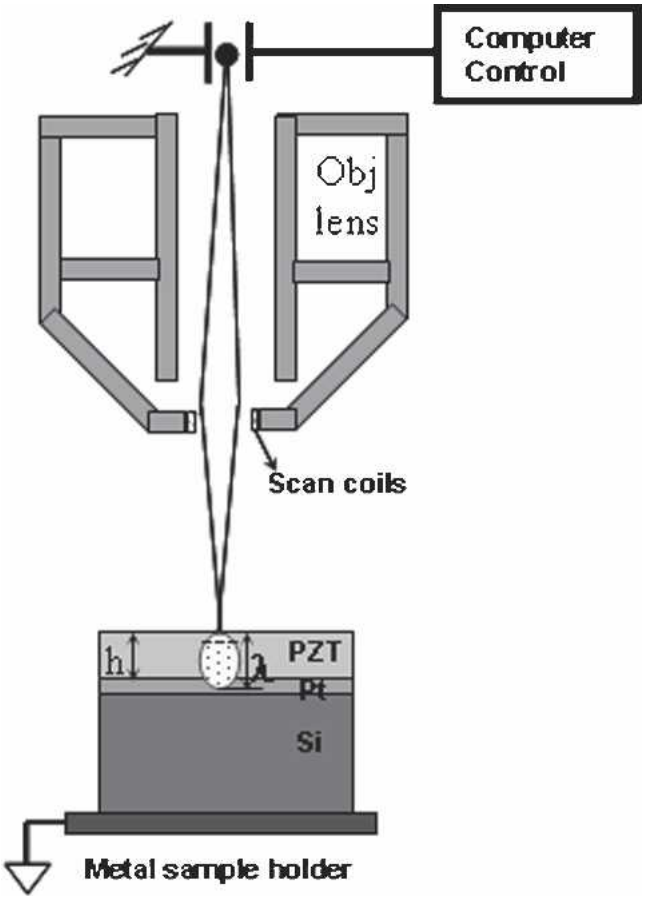


FIG. 1. Experimental setup for electron beam ferroelectric lithography and surface charge measurement. A scanning electron microscope equipped with lithography software is used to control the ferroelectric polarization by exposing the sample to a focused electron beam. Electrons penetrate the sample to a depth (λ) and develop the charges on ferroelectric surface. Electron penetration depth can be varied to be either greater or less than the film thickness (*h*) by changing the beam energy.

Domain polarization was quantified by PFM and scanning surface potential microscopy (SSPM). PFM imposes a small oscillating local electric signal on the surface and records the resulting piezoelectric deformation. The difference in phase between the imposed signal and deformation yields the domain orientation. A sinusoidal voltage with an amplitude of $V_{pp} = 5$ V and frequency of 70 kHz was applied to the Cr–Au coated atomic force microscope (AFM) tip. These conditions did not result in local domain switching, perhaps due to a local dielectric layer, which partially screens the effective electrical field between the tip and ferroelectric surfaces. The typical set-point voltage was 500 mV. The orientation and the magnitude of the electromechanical coupling coefficient were characterized by phase and amplitude signals, respectively.[14] In SSPM (also called Kelvin probe microscopy), a driving voltage of 2 V and a lift height of 40 nm were used. Nulling the force between the tip and sample yields the local surface potential. To quantitatively compare the domain surface potential resulting from different beam switching conditions, SSPM scan parameters were kept constant.

## III. RESULTS AND DISCUSSION

Figure 2 illustrates the process of charging and the underlying domain polarization reorientation in a PZT

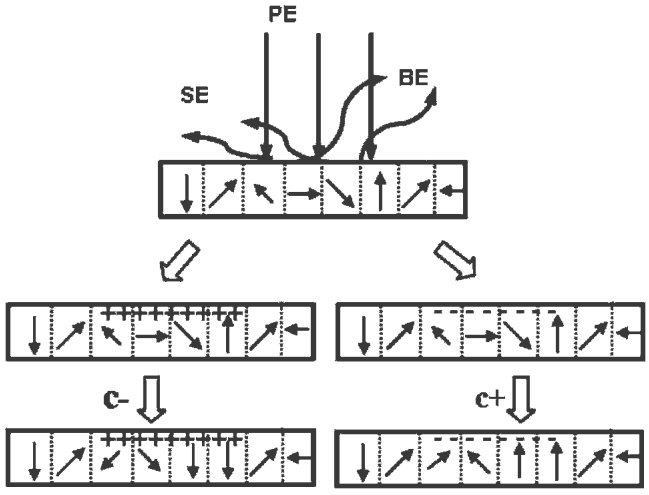


FIG. 2. Illustration of charging and polarization reorientation by an electron beam. Accumulation of positive charges causes the domains to point downwards (yielding the c– domains shown on the left). In contrast, negative charging leads to positive domain orientation (c+ domains on right). The schematic shows only the dominant charge and does not reflect the actual charge distribution in the film.

thin film under the electron beam irradiation. When positive net charging develops, polarization is reoriented such that a negative domain terminates the surface (often referred to as a c− domain). In contrast, negative net charging leads to positive domain orientation (c+ domains).

The dosage dependence of polarization switching is shown in Figs. 3(a) and 3(b). Figure 3(a) covers a range of exposures from 500 to ~5000 μC/cm$^2$. At each dosage level, the fraction of the irradiated area that is in the c+ orientation is determined from PFM images. Note in Fig. 3(b) that there is both a threshold dosage for the onset of switching and a saturation value at which the entire area is switched. At dosages below 500 μC/cm$^2$, no effect is observed; at dosages higher than 1500 μC/cm$^2$ all domains are reoriented. Between these values, there is a monotonic increase in the switched area.

In our films, the grains differ somewhat in size and in orientation with respect to the surface. The majority of grains are of a single domain; the small size makes multidomains unlikely. A reasonable explanation for the observed behavior rests on the orientation differences. When the local electric field reaches the critical value, domains with the most favorable polarization orientation switch. The polarization switching process is schematically shown in the Fig. 3(c). The dosage dependence could be related to the orientation dependence in nucleation or in domain wall motion. These critical dosages will also likely vary with several film parameters that are not investigated in our study; such as crystallinity, thickness, conductivity, and defect concentration.

The local electric field in the film stems from the charge buildup in the PZT caused by the irradiating electron beam. The net charge buildup is determined by the interplay between the charge flow (i.e., current) of the emitted secondary electrons ($I_S$), the backscattered electrons ($I_B$), and the leakage current ($I_L$), to the primary beam current ($I_0$):

$$\sigma = \frac{I_B + I_S + I_L}{I_0} \quad , \tag{1}$$

where σ is the electron emission yield depending on beam energy and $I_0$ that determines the net charging (where $I_B + I_S + I_L$ is not simply proportional to $I_0$).[15] The builtup charge in the dielectric can be accommodated by the defects in the dielectric medium, which act as charge traps.[16] It is difficult to determine the exact charge profile, with both positive and negative net charges have been reported in dielectrics.[15] As the charge builds up, this will lead to an induced electric field determined by the positively and negatively charged regions, and the capacitive interaction with the conducting ground plane. Positive charge is expected in a thin (<50 nm) layer close to the surface due to secondary electron emission, while a more disperse negative charge is expected from the trapping of electrons down to the penetration depth.[17] At the interface of the positive and negative charged region, a large electric field is developed, which can cause the dielectric to be poled in the downward direction (see Fig. 2). When the total negative charge is much larger than the positive, the system can be

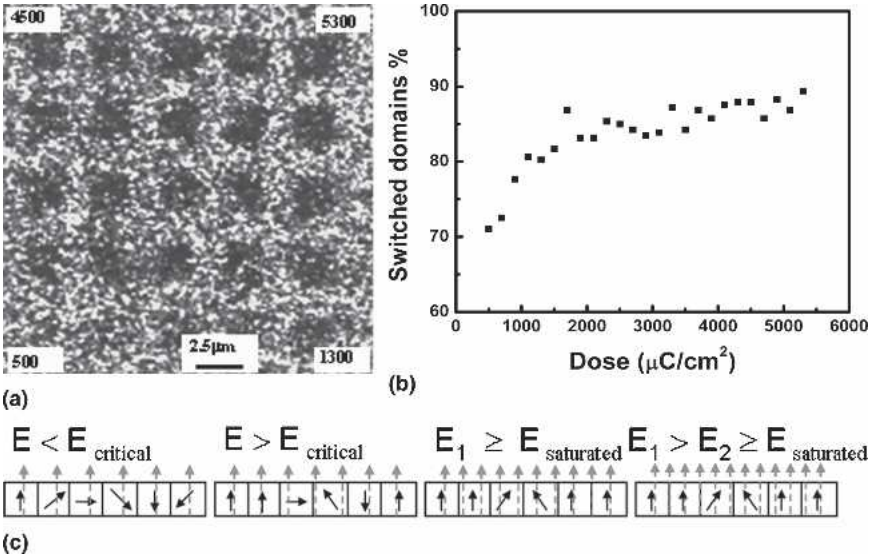


FIG. 3. (a) PFM phase image (over 20 × 20 μm area, from Ref. 8) showing negative domain polarization switched by $E = 10$ keV, $I = 30$ pA, and dosages ranging from ~500 to 5000 μC/cm$^2$. The exposure is increased from left to right and from bottom to top in the figure with the dosage values (in μC/cm$^2$) indicated for the corner positions. The darker regions are the negatively polarized domains. (b) The fraction of c− domains switched perpendicularly to the surface, as determined by a bearing analysis, increases with electron dosage (from Ref. 8). (c) Model of domain switching with electric field ($E$) as dashed arrows. For $E$ greater than $E_{critical}$, the domains begin switching. The fraction of switched domains increases with electron dose until the reorientation saturates at 1500 μC/cm$^2$, as in (b).

approximated as a uniformly negatively charged cylinder. Cazaux has worked out the details of the resulting surface potential in a bulk dielectric material with a uniform charge distribution[17,18]

$$V_S = \frac{Q_T}{\pi\epsilon_0(1+\epsilon_r)a} \quad , \tag{2}$$

where $Q_T$ is the total trapped charge in the volume, $\epsilon_r$ is the relative permittivity of the material, and $a$ is the spot diameter of electron beam. This can be extended to the case of dielectric thin film on a metallic substrate, which takes into account the image charge in the substrate and gives to first order the surface potential[19]

$$V_S = \frac{Q_T}{\pi\epsilon_0(1+\epsilon_r)a} f \quad , \tag{3}$$

where $f$ is a complex factor between 0 and 1 that accounts for the geometry of the thin film. Though charge trapping in dielectrics is complex with the concentration varying considerably with sample, we can attempt an estimate of the induced field with Eq. (3) for a typical polycrystalline sample when negative charging is dominant. If the sole mechanism of electron trapping in the PZT were due to intrinsic defects, and a reasonable defect density is assumed ($\sim 10^{20}/cm^3$),[16] the resulting surface potential would be estimated to be less than 51 mV. Over a film thickness of 160 nm, this corresponds to an electric field of 3.2 kV/cm, which is below the coercive field (~30–100 kV/cm) typically found for PZT. Since the domains do, in fact, switch, additional charge may be trapped by other mechanisms or reside in the film as a transient charge buildup that slowly dissipates away by electrical conduction as a leakage current. A possible explanation for this slight underestimate for the induced field may stem from defects not accounted for, induced by e-beam irradiation during exposure, which in turn could permit an increased internal electrical field in the film.

Despite the above underestimate of the induced electric field, comparison to charging in single crystalline dielectric material is in rough agreement. Using a typical coercive field value of 100 kV/cm for PZT, we can calculate the necessary surface charge density from Eq. (3), which yields 200 $\mu C/cm^2$. This is slightly less than the measured (500 $\mu C/cm^2$) critical dosage applied by the SEM, which gives a value for $\sigma$ of about 3/5. This value of $\sigma$ is in reasonable (order of magnitude) agreement with the reported charging of single crystal dielectrics in Ref. 18.

To determine the relationship between beam energy and polarization reorientation, the PZT sample was irradiated with the electron beam at various energies $E$, ranging from 1 to 30 keV at a constant dosage of 3000 $\mu C/cm^2$ and beam current of 1 nA. Figure 4(a) shows the surface potential variation of switched regions in a SSPM phase image. In Fig. 4(b), the degree of polarization reorientation is quantified. The magnitude of the surface potential measured in ambient is not that of the polarization charge because adsorbates compensate the charge at the surface. However the relative differences in potential contrast are directly related to the area of switched domains, a result confirmed by PFM. The monotonic variation of polarization switching with beam energy at 1 nA is clear in Fig. 4(b).

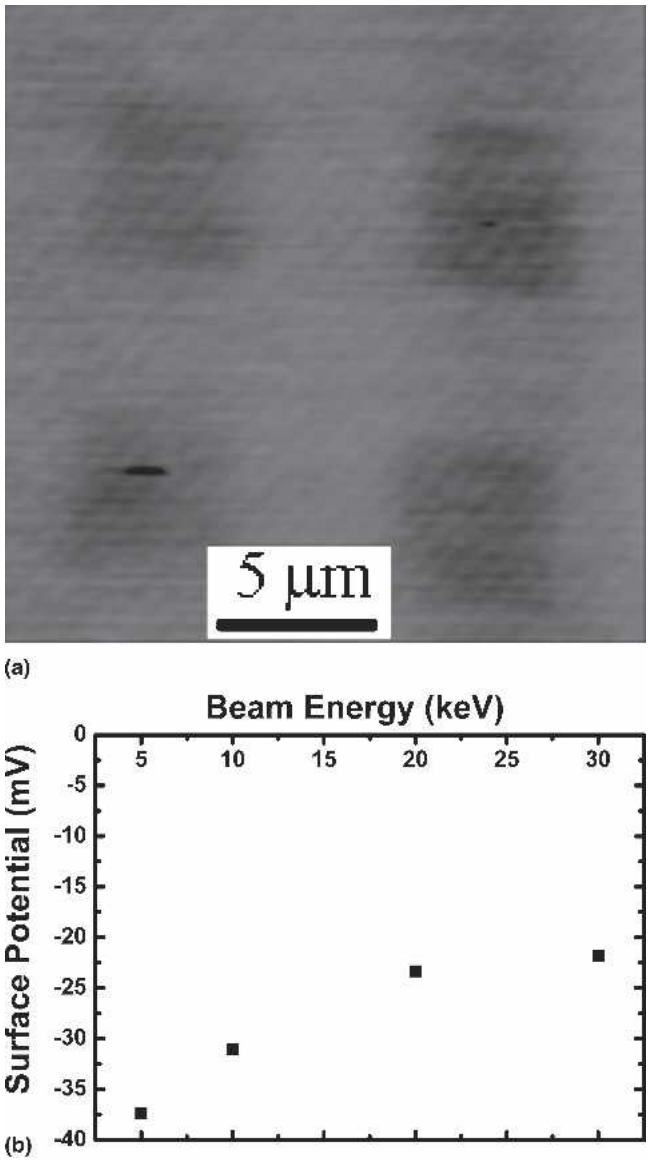


FIG. 4. (a) A SSPM phase image showing that compensating surface charges are negative and that the corresponding domains are c+. This pattern was written with 3000 $\mu C/cm^2$, 1 nA, and 10 keV. (b) Domain surface potential exhibits energy dependence at constant beam current of 1 nA and constant dosage of 3000 $\mu C/cm^2$.

The beam current dependence of the domain reorientation is illustrated in Fig. 5, which demonstrates that switching to both positive and negative orientations is possible. In this figure, the sign and relative amplitude of

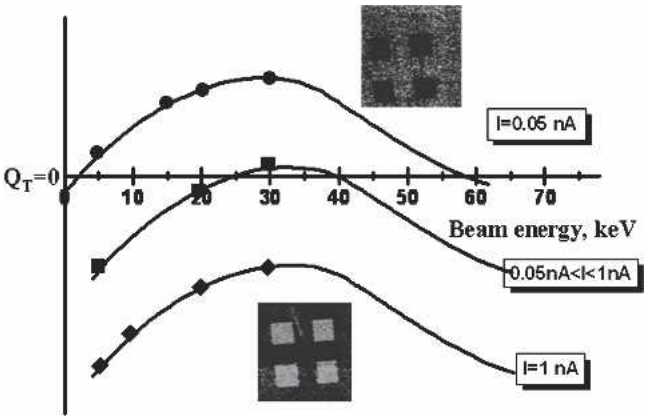


FIG. 5. Polarization reorientation dependence on beam energy and current. Dots represent experimental determination of domain polarity [such as in Fig. 4(b)] superimposed on a schematic representation of $Q_T$, which should follow the expected trend of the total electron emission yield σ for an insulator. The intercept along the *y*-axis represents $Q_T = 0$, which corresponds to σ equal to 1. At high beam current (>1 nA), a net negative charge accumulates in the film, which switches the underlying domains in the positive direction (c+). At low beam current (<50 pA), positive charges are more dominant, resulting in negative domain polarization (c−). For beam currents between 50 pA and 1 nA, the sign of net charge depends on beam energy. (Insets) PFM phase images showing (bottom) positive polarization from a 1 nA beam and (top) negative polarization from a 0.05 nA beam, switched with 3000 μC/cm$^2$ and 30 keV. The small square patterns are 5 × 5 μm.

net charge, which was provided by polarity of switched domains, shows dependences on both beam current and energy. At beam currents <0.5 nA, net charge is positive under all conditions and domains reorient with c− termination. At currents >1 nA the net charge is negative, resulting in c+ surface domains. At intermediate currents, the sign of the charge and induced domain polarization depends on the beam energy.

The energy dependence of the electron penetration depth is given by the Kanaya–Okayama range relation[20]

$$\lambda = \frac{0.0276AE^{1.67}}{Z^{0.89}d} \quad , \tag{4}$$

where $A$ is the atomic weight in grams per mol, $E$ is electron beam energy in keV, $Z$ is the average atomic number, and $d$ is the density in g/cm$^3$, ($A = 235$ g/mol, $Z = 63$, and $d = 7.5$ g/cm$^3$ for PZT). The penetration depths for various beam energies are listed in Table I. For thin films with the thickness of $h$, when $\lambda > h$, some fraction of the electrons will contribute to the leakage current through the Pt film and the silicon substrate (see Fig. 1). For beam energies higher than 3.8 keV, the penetration depth of the incident electrons exceeds the PZT film thickness of 160 nm. With electron beam energies less than 3.8 keV, a substantial number of the electrons should be trapped within the film. At beam energies above ~10 keV, substantial numbers of electrons enter the underlying Pt/Si substrate. The excitation cross sections that result in electron emission at the surface, $I_B$ and $I_S$, also scale with the beam energy. Thus, as beam energy increases, more electrons are lost at the surface, and the PZT film should be less negatively charged.

TABLE I. Electron penetration depth in polycrystalline PZT.

| E (keV) | Penetration depth (nm) |
|---|---|
| 1 | 21.7 |
| 3.8 | 200 |
| 5 | 318 |
| 10 | 1013 |
| 20 | 3222 |
| 30 | 6316 |

The net charge in the dielectrics typically exhibits the behavior superimposed schematically as dashed lines on the data in Fig. 5. The behavior of the net charge should closely follow the behavior of σ as a function of beam current and energy. At low beam energy, as the excitation cross section increases with beam energy, σ generally increases, which results in the net charge becoming more positive. At higher beam energies, the number of electrons that are stopped within the depth of the PZT film decreases (as the penetration depth increases), and σ will decrease leading to decreasing $Q_T$. The combination of these two effects results in a maximum of σ and $Q_T$ for a given beam current. Evidence for the increasing $Q_T$ regime at lower energies is seen through the SSPM and PFM data. PFM measurements were used to determine the sign of the polarization (and thus $Q_T$) in Fig. 5, yet they do not give clear information on the overall magnitude of the polarization as a function of beam energy and current due to the difficulty of varying these parameters over the course of an electron beam write. For the data in the negative charging region of Fig. 5, the SSPM measurements yielded curves similar to Fig. 4(b), which suggests the trend schematically represented in Fig. 5. These studies did not determine the high energy cross over to $\sigma < 1$, indicating that the crossover energy is above that accessible by our SEM. The surface potential of the reoriented PZT domains exhibits similar beam current dependence to those of $Al_2O_3$ and $ZrO_2$ irradiated with a high beam current density.[15] Additionally, the current dependence indicates that the negative charging process is a dynamic competition between secondary electron emission and surface electron trapping.

These results are summarized in Table II. At low current density (10$^6$ pA/cm$^2$), polarization is always reoriented negatively, implying a positive charge. At high current density (10$^9$ pA/cm$^2$), the same beam dosage and energies yield positively switched polarization. As noted above, the concentration of intrinsic defects is not sufficient to cause the negative charge necessary for polarization switching. Consequently, a more complex electron

TABLE II. Surface charging and polarization reorientation under different electron irritation conditions.

| Sample number | Beam energy (keV) | Beam current (nA) | Total exposure time | Sign of surface charge | Polarization direction |
|---|---|---|---|---|---|
| 1 | 5 | 0.05 | 2 min | + | − |
| 2 | 5 | 1 | 2 min | − | + |
| 3 | 5 | 4.8 | 2 min | − | + |
| 4 | 10 | 0.05 | 2 min | + | − |
| 5 | 10 | 10 | 2 min | − | + |
| 6 | 20 | 0.05 | 2 min | + | − |
| 7 | 20 | 1 | 2 min | − | + |
| 8 | 20 | 10 | 2 min | − | + |
| 9 | 30 | 0.05 | 2 min | + | − |
| 10 | 30 | ~0.9 | 18 s | + | − |
| 11 | 30 | 20 | 2 min | − | + |

interaction that results in electron trapping at the surface must be occurring at high current densities.

## IV. CONCLUSIONS

We have demonstrated an effective method to switch ferroelectric polarization in polycrystalline PZT thin films by e-beam lithography. Under various exposure conditions, both positively and negatively poled features can be created. With electron injection, trapped charge develops, establishing a local electrical field, which switches the underlying polarization when sufficiently high. Due to the length scale accessible to conventional e-beam tools, this method provides the opportunity for domain engineering at the nanometer scale.

## ACKNOWLEDGMENTS

The authors acknowledge the support from NIRT, Nano/Bio Interface Center (NBIC) Grant No. DMR03-04531.

## REFERENCES

1. J.F. Scott and C.A.P. De Araujo: Ferroelectric memories. *Science* **246,** 1400 (1989).
2. K. Uchino: *Ferroelectric Devices* (Marcel Dekker, New York, 2000).
3. S.V. Kalinin, D.A. Bonnell, T. Alvarez, X. Lei, Z. Hu, and J.H. Ferris: Atomic polarization and local reactivity on ferroelectric surfaces: A new route toward complex nanostructures. *Nano Lett.* **2,** 589 (2002).
4. S.V. Kalinin, D.A. Bonnell, T. Alvarez, X. Lei, Z. Hu, R. Shao, and J.H. Derris: Ferroelectric lithography of multicomponent nanostructures. *Adv. Mater.* **16,** 795 (2004).
5. M. Yamada, N. Nada, M. Saitoh, and K. Watanabe: First-order quasi-phase matched $LiNbO_3$ waveguide periodically poled by applying an external field for efficient blue second-harmonic generation. *Appl. Phys. Lett.* **62,** 435 (1993).
6. C.H. Ahn, T. Tybell, L. Antognazza, K. Char, R.H. Hammond, M.R. Beasley, O. Fischer, and J-M. Triscone: Local, nonvolatile electronic writing of epitaxial $Pb(Zr_{0.52}Ti_{0.48})O_3/SrRuO_3$ heterostructures. *Science* **276,** 1100 (1997).
7. T. Tybell, C.H. Ahn, and J-M. Triscone: Control and imaging of ferroelectric domains over large areas with nanometer resolution in atomically smooth epitaxial $Pb(Zr_{0.2}Ti_{0.8})O_3$ thin films. *Appl. Phys. Lett.* **72,** 1454 (1998).
8. J.H. Ferris, D.B. Li, S.V. Kalinin, and D.A. Bonnell: Nanoscale domain patterning of zirconate titanate materials using electon beams. *Appl. Phys. Lett.* **84,** 774 (2004).
9. M. Yamada and K. Kishima: Fabrication of periodically reversed domain structure for SHG in $LiNbO_3$ by direct electron-beam lithography at room temperature. *Electron. Lett.* **27,** 828 (1991).
10. J. He, S.H. Tang, Y.Q. Qin, P. Dong, H.Z. Zhang, C.H. Kang, W.X. Sun, and Z.X. Shen: Two-dimensional structures of ferroelectric domain inversion in $LiNbO_3$ by direct electron-beam lithography. *J. Appl. Phys.* **93,** 9943 (2003).
11. D.C. Joy: Database on electron-solid interactions (private communication, 2001).
12. Y. Xu: *Ferroelectric Materials and Their Applications* (North-Holland, New York, 1991), p. 110.
13. MCNC, Raleigh, NC, composition specified by the vendor.
14. S.V. Kalinin and D.A. Bonnell: Imaging mechanism of piezoresponse force microscopy of ferroelectric surfaces. *Phys. Rev. B* **65,** 125408 (2002).
15. S. Fakhfakh, O. Jbara, M. Belhaj, Z. Fakhfakh, A. Kallel, and E.I. Rau: Dynamic investigation of electron trapping and charge decay in electron-irradiated $Al_2O_3$ in a scanning electron microscope: Methodology and mechanisms. *Nucl. Instrum. Meth. B,* **197,** 114 (2002).
16. R. Renoud, F. Mady, and J-P. Ganachaud: Monte Carlo simulation of the charge distribution induced by a high-energy electron beam in an insulating target. *J. Phys. Condens. Matter* **14,** 231 (2002).
17. J. Cazaux: Some considerations on the electric field induced in insulators by electron bombardment. *J. Appl. Phys.* **59,** 1418 (1986).
18. T. Thome, D. Braga, and G. Blaise: Effect of current density on electron beam induced charging in sapphire and yttria-stabilized zirconia. *J. Appl. Phys.* **95,** 2619 (2004).
19. R. Coelho, B. Aladeniz, B. Garros, D. Acroute, and P. Mirebeau: Toward a quantitative analysis of the mirror method for characterizing insulation. *IEEE Tran. Dielectr. Electr. Insul.* **6,** 202 (1999).
20. K. Kanaya and S. Okayama: Penetration and energy-loss theory of electrons in solid targets. *J. Phys. D* **5,** 43 (1972).